

G.J. Kramer, G.Y. Fu, R. Nazikian, R.V. Budny, C.Z. Cheng, N.N. Gorelenkov,
S.D. Pinches, S.E. Sharapov, K-D. Zastrow and JET EFDA contributors

Reversed Shear Alfvén Eigenmodes in the Frequency Range of the Triangularity Induced Gap on JET

“This document is intended for publication in the open literature. It is made available on the understanding that it may not be further circulated and extracts or references may not be published prior to publication of the original when applicable, or without the consent of the Publications Officer, EFDA, Culham Science Centre, Abingdon, Oxon, OX14 3DB, UK.”

“Enquiries about Copyright and reproduction should be addressed to the Publications Officer, EFDA, Culham Science Centre, Abingdon, Oxon, OX14 3DB, UK.”

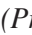
Reversed Shear Alfvén Eigenmodes in the Frequency Range of the Triangularity Induced Gap on JET

G.J. Kramer¹, G.Y. Fu¹, R. Nazikian¹, R.V. Budny¹, C.Z. Cheng², N.N. Gorelenkov¹,
S.D. Pinches³, S.E. Sharapov³, K-D. Zastrow³ and JET EFDA contributors*

¹*Princeton Plasma Physics Laboratories, P.O. box 451, Princeton, New Jersey 08543*

²*Plasma and Space Science Center, National Cheng-Kung University, Tainan, Taiwan*

³*Euratom/UKAEA Fusion association, Culham Science Centre, Abingdon, OX14 3DB, UK*

* See annex of M.L. Watkins et al, "Overview of JET Results",
(Proc.  IAEA Fusion Energy Conference, Chengdu, China (2006)).

ABSTRACT

Reversed shear Alfvén eigenmodes in the non-circular triangularity induced Alfvén eigenmode frequency range are observed during the current ramp-up phase in JET discharges. Ideal magnetohydrodynamical calculations are able to reproduce the observed Alfvén eigenmode spectra accurately. It was found that these modes come into existence because of the plasma elongation.

In reversed magnetic shear discharges in tokamaks Alfvén eigenmodes are often observed that reside near the shear reversal point, the Reversed shear Alfvén Eigenmodes (RSAE) and they are seen in most large tokamaks [1-5]. They consist of one dominant poloidal harmonic and chirp up in frequency because the minimum magnetic safety factor, q_{\min} , is decreasing in time [6]. The RSAEs, which are sometimes called Alfvén cascades, have a minimum frequency close to the Geodesic Acoustic Mode [7] and chirp up to the TAE frequency and therefore they are associated with the TAE gap. These modes are located just above the (local) maximum in the Alfvén continuum at q_{\min} .

In modern tokamaks the plasma cross section is not circular but highly shaped to stabilize low-frequency MHD activity but this shaping opens up higher frequency gaps in the Alfvén spectrum. The Ellipticity induced Alfvén Eigenmode (EAE) gap opens at about twice the TAE frequency because of the plasma ellipticity while the Non-circular triangularity induced Alfvén Eigenmode (NAE) gap opens at three times the TAE frequency because of the plasma triangularity.

In all those Alfvén Eigenmode (AE) gaps eigenmodes can reside which can be excited easily by a population of fast ions in the plasma. In a burning tokamak plasma the 3.5MeV fusion-born alpha particles should deposit their energy first in the plasma core to sustain the burn before they got lost. The magnetic perturbations due to the Alfvén eigenmodes can transport the alpha particles from the plasma core before they are thermalized with the bulk plasma thereby reducing the efficiency of the burn [8]. It is therefore important study these AEs on present machines and model them accurately so that predictions can be made about fast alpha particle losses in burning plasmas for ITER and device ways to suppress harmful AE activity.

Local maxima in the Alfvén continuum at the shear reversal point, similar to the one in the TAE gap where the RSAE exist, are also present in the higher gaps (see Fig.1). In a recent paper [9] simulations indicated and analytical theory confirmed that RSAEs can exist in the EAE, NAE, and higher order gaps. In this paper we report on the observation of RSAEs in the NAE gap in discharges in the Joint European Torus, JET. The modes were found during the current ramp-up phase of discharges created to study high triangularity internal transport barrier scenarios. After reviewing the RSAE theory briefly we show the experimental evidence for NAE-RSAEs and identify the modes from detailed MagnetoHydroDynamical (MHD) simulations.

Within the framework of a reduced MHD model for the shear Alfvén waves in a low-beta plasma and a linearized momentum equation a criterion for the existence of the RSAEs associated with the TAE gap can be obtained [10, 11]. It was show in [10, 11] that RSAEs in the TAE gap can exist with zero pressure gradient but that a finite pressure gradient contributes favorably to the mode existence

as was found earlier from simulations [12]. An analytic criterion for the existence of RSAEs localized near q_{\min} for large-aspect ratio finite-beta tokamaks with circular flux surfaces was derived in [6] as $Q > 1.4$ and in various papers Q is calculated with different assumptions for the plasma and/or fast-ion contributions [6, 7, 10, 11].

An analytical existence criterion for RSAEs in the TAE, EAE, NAE, and higher order gaps was given in [9] as:

$$Q = \frac{-mq_{\min}^2 k_m}{r_{\min}^2 q_{\min}''} \left(\frac{3\epsilon^2 - \alpha^2 + 2\epsilon\alpha(1+2(1-q_{\min}^{-2})(2k_m q_{\min})^{-2} - 1))}{1-(2k_m q_{\min})^2} \right) \quad (1)$$

where the terms up to quadratic in the pressure gradient were included. In the above expression $\epsilon = r_{\min}/R_0$ is the inverse aspect ratio (R_0 the major radius), $\Delta' = d\Delta/dr$ is the derivative of the Shafranov shift, Δ , $\alpha = -(R_0 q_{\min}^2/B^2)dP/dr$, with P the plasma pressure and B the magnetic field strength, $q_{\min}'' = d^2q/dr^2$ evaluated at r_{\min} , the location of q_{\min} and $k_m = n - m/q_{\min}$ the normalized parallel wave number with n the toroidal and m the poloidal mode number.

For the up-chirping RSAEs in the TAE gap, when q_{\min} decreases, k_m changes from zero at the rational q surface, m/n , to $-1/2q_{\text{TAE}}$ when the RSAE changes into a TAE at $q_{\text{TAE}} = (m-1/2)/n$ and hence Q is positive for TAE-RSAEs under the condition for which Eq.1 was derived: $\beta \sim O(\epsilon^2)$ or equivalently, α is small. For RSAEs associated with higher order gaps k_m is less than minus one which means that the term: $1-(2k_m q_{\min})^2$ is negative. The existence condition (Eq.1) can only be fulfilled when the term: $3\epsilon^2 - \alpha^2 + 2\epsilon\alpha(1+2(1-q_{\min}^{-2})(2k_m q_{\min})^{-2} - 1))$ is negative. This condition is only fulfilled when α exceeds a critical value as was shown in [9].

In the derivation of eq.1 a circular plasma cross section was taken and the theory was used to benchmark ideal MHD simulations successfully [9]. In most large tokamaks, however, D-shaped plasmas are used. In order to make an accurate comparison between experiment and theory we have used the Non-Variational ideal MHD code NOVA [13, 14] in which the full plasma geometry is used together with compressibility effects and no restrictions on α . From these simulations we have found that apart from pressure gradient effects the ellipticity, κ , is a major contributor to the existence of the RSAEs in the NAE gap as can be seen from Fig.2. At small values of κ the NAE-RSAE only comes into existence when α is sufficiently high which is in accordance with the above theory. At large values of κ the NAE-RSAE exists even when α is zero i.e. the plasma elongation is increasing Q to above its critical value. The effect of κ to the mode structure is a coupling between two poloidal harmonics m and $m-2$ as can be seen in figs. 2b and c. When q_{\min} decreases and the NAE-RSAE chirps up to the NAE gap the mode evolves into a proper NAE whereby the $m-2$ harmonic decreases and the $m-3$ harmonic becomes of the same size as the m component.

RSAEs in the NAE gap were observed in the pre-heat phase during the current ramp up of discharges in JET that were created to study high triangularity internal transport barrier scenarios. The plasma had the following geometrical parameters: major radius, $R_0 = 2.91\text{m}$, minor radius, $r = 0.94\text{m}$, elongation, $\kappa = 1.77$, triangularity, $\delta = 0.3$, and a toroidal magnetic field of 3.1T . Time

traces of the main plasma parameters are shown in Fig.3 and the magnetic fluctuations in Fig.4. Density profiles were obtained from multi- chord interferometry while ECE data was used for the temperature profiles. The q profile was obtained from an equilibrium reconstruction with EFIT [15] and was independently verified from the observed RSAE activity in the TAE gap (see below).

In the spectrum shown in Fig.4 the RSAE activity associated with the TAE gap is clearly visible between 30 and 130kHz while AE activity at the bottom and the top of the EAE gap is present around 170 to 210kHz and 240 to 280kHz respectively. Between 300 and 340 kHz $n = 2$ RSAEs associated with the NAE gap are visible. They behave very similar as the $n = 2$ RSAEs in the TAE gap as expected from theory. These modes are not a harmonic of the $n = 2$ TAE-RSAE because the mode frequency is not an exact multiple of the TAE-RSAE frequency. Poloidal mode number measurements indicate that during the up-chirp m is one larger for those NAE-RSAEs than for the $n = 2$ TAE-RSAEs which is also in agreement with poloidal mode number predictions from theory.

In order to explain the measured fluctuation spectrum more completely, ideal MHD simulations were performed with the NOVA code from 1.35 to 3.00 s with 10 ms time steps. The equilibrium parameters were obtained from a TRANSP analysis [16] based on experimental parameters together with an EFIT equilibrium reconstruction of the q profile. The magnetic shear is very low over a large region of the plasma during the current ramp-up phase as is shown in Fig.5 and the shear-reversal point is located at about half the minor radius, creating favorable conditions for the existence of RSAEs in the TAE and NAE gaps.

The evolution of q_{\min} was verified independently from the observed time history of the TAE-RSAEs. In Fig.6 it can be seen that before 1.8s q_{\min} from the EFIT equilibrium reconstruction follows accurately q_{\min} as obtained experimentally from MHD spectroscopy but at later times, when the RSAE activity is strong, the EFIT q_{\min} is systematically lower by about 0.12 than the one deduced from TAE-RSAE spectroscopy. Because the RSAE frequency evolution depends very sensitively on q_{\min} we have shifted the results of the simulations as shown in fig.7 by up to 80ms so that q_{\min} in the simulations line up with the measured values.

For an accurate calculation of RSAE frequencies the plasma compressibility has to be taken into account [7, 17] and in the current NOVA simulations we have used the canonical value of 5/3 for the adiabatic index of compression, γ , together with the filtering technique as described in [18] to eliminate spurious solutions. Scanning γ from 1.0 to 2.0 for an $n = 1$ TAE-RSAE, the mode that is the most sensitive to gamma [17], near its minimum frequency at 2.6s revealed that the eigen frequency varied by less than 10 kHz indicating that the results are not very sensitive to the exact value of γ .

From the very good agreement between the measured and simulated frequency behaviour of the TAE-RSAEs and the NAE-RSAEs we conclude that we have positively identified the NAE-RSAEs. In the simulations, however, NAE-RSAEs are found to exist before they appear experimentally. This can be explained by the fact that the damping is the strong near the bottom of the frequency chirp and decreases when the mode moves up in frequency into the NAE gap. A complete stability

analysis is beyond the scope of this paper. For the identification of the NAE-RSAEs toroidal mode numbers were important for the simulations and therefore the observation of those modes on Mirnov coils was crucial. Mirnov coils are not sensitive to high- n modes that are located well inside the plasma and other experimental techniques should be used to detect the high- n RSAEs [5, 19].

In the EAE gap the simulated modes at the top also agree well with the observed ones. These are EAEs that emerge from the Alfvén continuum when the tip of the continuum reaches a resonant q surface for an EAE. The agreement between the simulations and the experiment of the EAEs at the bottom of the EAE gap is somewhat less. In the simulations the upper EAE is located at $r/a = 0.7$ whereas the lower EAE is located at $r/a = 0.3$ (see fig.1a). Experimental uncertainties of the profiles in the core might explain the differences between the observed and simulated frequency behavior of the EAEs near the bottom of the EAE gap.

In summary, RSAEs associated with the NAE gap which were predicted to exist based on ideal MHD simulations and analytical theory have been observed in the current ramp-up phase of JET discharges. Simulated eigenmode spectra with toroidal mode numbers one, two, and three agreed very well with the observed spectra. From this agreement RSAEs associated with the NAE gap were positively identified. Additional experimental evidence on poloidal mode numbers indicated that during the up-chirp, when the RSAE consists of one dominant poloidal harmonic, the m -number of the NAE-RSAE is one higher than the m -number of the TAE-RSAE which is also in agreement with theory. Previously it was found that NAE-RSAEs can only exist in plasmas with circular cross sections when the normalized pressure gradient, β_p , is above a certain threshold. For D-shaped plasmas, however, we have found that the plasma elongation contributes favorably to the existence criterion of the NAE-RSAEs and therefore, the NAE-RSAEs cannot be suppressed by reducing the pressure gradient in the vicinity of q_{min} where the NAE-RSAEs reside in elongated tokamak plasmas.

ACKNOWLEDGEMENTS

This work has been conducted under DOE Contract No. DE-AC02-76-CH0373 and under the JET-EFDA workprogramme. Therefore, the authors thank all the contributors to the experimental campaigns and tokamak maintenance.

REFERENCES

- [1]. Y. Kusama et al., Nucl. Fusion **38** 1215 (1998).
- [2]. J.A. Snipes et al., Plasma Phys. Contr. Fusion **42** 381 (2000).
- [3]. S.E. Sharapov et al., Phys. Lett. A **289** 127 (2001).
- [4]. R. Nazikian et al., Phys. Rev. Lett. **91** 125003 (2003).
- [5]. R. Nazikian et al., Phys. Rev. Lett. **96** 105006 (2006).
- [6]. H.L. Berk et al., Phys. Rev. Lett. **87** 185002 (2001).
- [7]. B.N. Breizman et al., Phys. Plasmas **11** 4939 (2005).

- [8]. G-Y. Fu and J.W. Van Dam, Phys. Fluids B **1** 1949 (1989).
 [9]. G.J. Kramer and G-Y. Fu, Plasma Phys. Contr. Fusion **48** 1285 (2006).
 [10]. G.Y. Fu and H.L. Berk, Phys. Plasmas **13** 052502 (2006).
 [11]. N.N. Gorelenkov, G.J. Kramer, and R. Nazikian, Phys. Contr. Fusion **48** 1255 (2006).
 [12]. G.J. Kramer et al., Plasma Phys. Contr. Fusion **46** L23 (2004).
 [13]. C.Z. Cheng and M.S. Chance, Journ. Comp. Phys. **71** 124 (1987).
 [14]. C.Z. Cheng, Phys. Rep. **211**, 1 (1992).
 [15]. L.L. Lao et al., Nucl. Fusion **30**, 1035 (1990).
 [16]. R.V. Budny, et al., Nucl. Fusion **35**, 1497 (1995).
 [17]. G.J. Kramer, et al., Phys. Plasmas **13** 056104 (2006).
 [18]. M. Chu et al., Phys. Fluids B **4** 3713 (1992).
 [19]. S.E. Sharapov et al., Phys. Rev. Lett. **04** 165001 (2004).

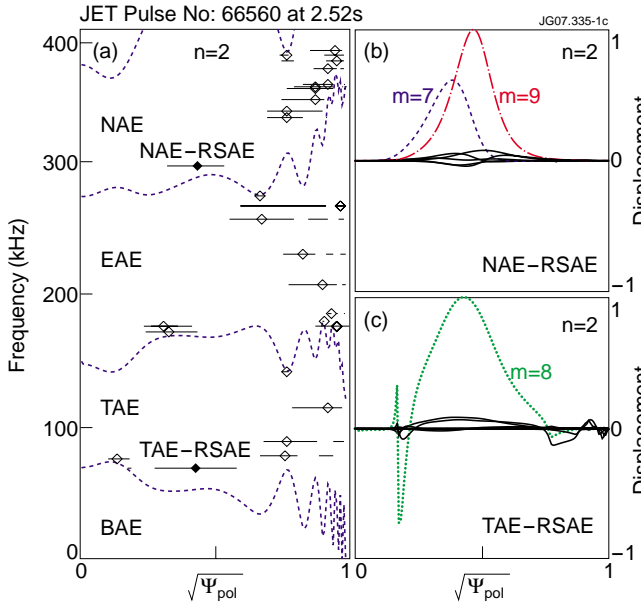


Figure 1: (a) Alfvén continuum with conventional Alfvén eigenmode solutions (open diamonds) and the RSAE in the TAE and NAE gap (black diamonds) as function of the normalized poloidal flux coordinate ($\sqrt{\Psi_{pol}}$ r/a). (b) The TAE-RSAE and (c) the NAE-RSAE structure.

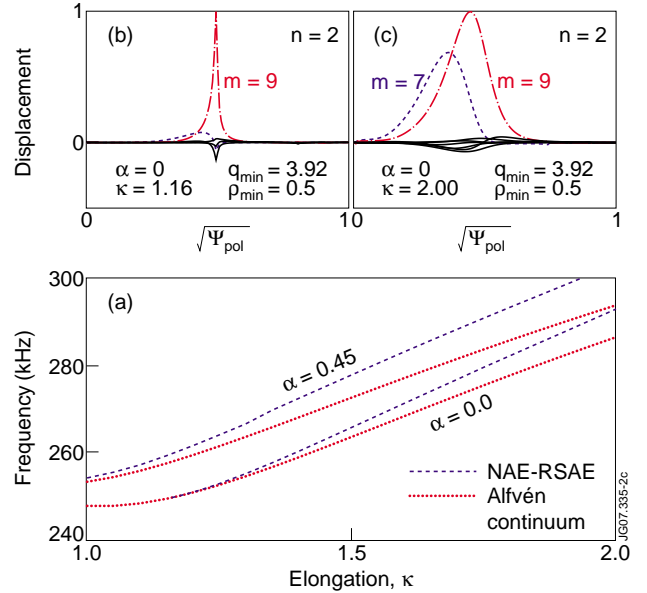


Figure 2: (a) NAE-RSAE frequency as function of κ for two values of α . At low α 's the mode only exists when κ is large enough while at high α 's the mode exist even for circular cross sections. (b) NAE-RSAE structure when it just emerges from the continuum and (c) at a large value of ($\sqrt{\Psi_{pol}} \approx r/a$).

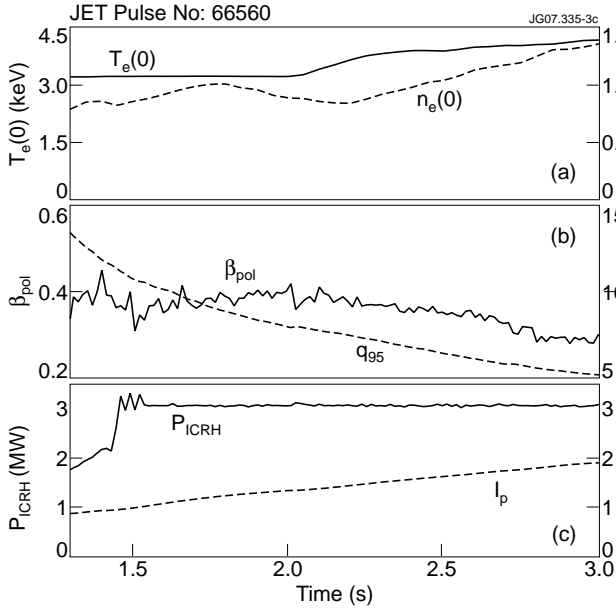


Figure 3: Time traces of (a) the central electron temperature, $T_e(0)$, and density, $n_e(0)$, (b) the poloidal beta, β_{pol} and the magnetic safety factor at $r/a = 0.95$, q_{95} , and (c) the heating power, P_{ICRH} and plasma current, I_p .

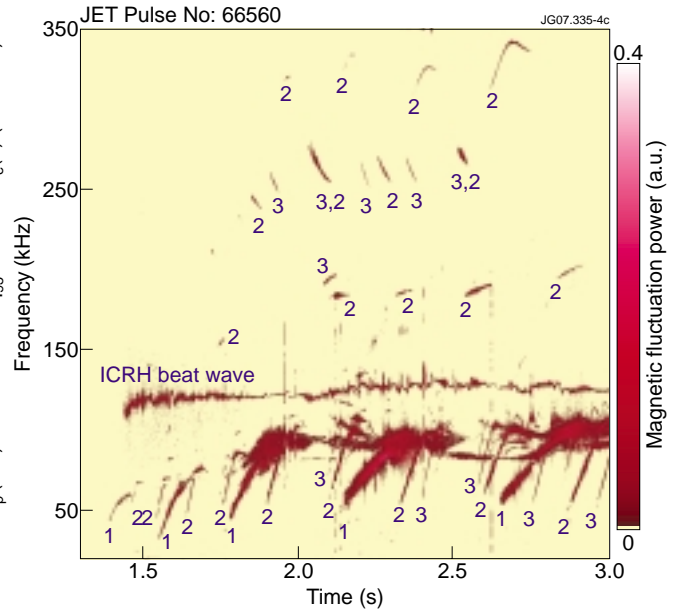


Figure 4: Magnetic fluctuation spectrum with the AEs indicated with their toroidal mode number. The NAE-RSAE activity is clearly visible between 300 and 350kHz.

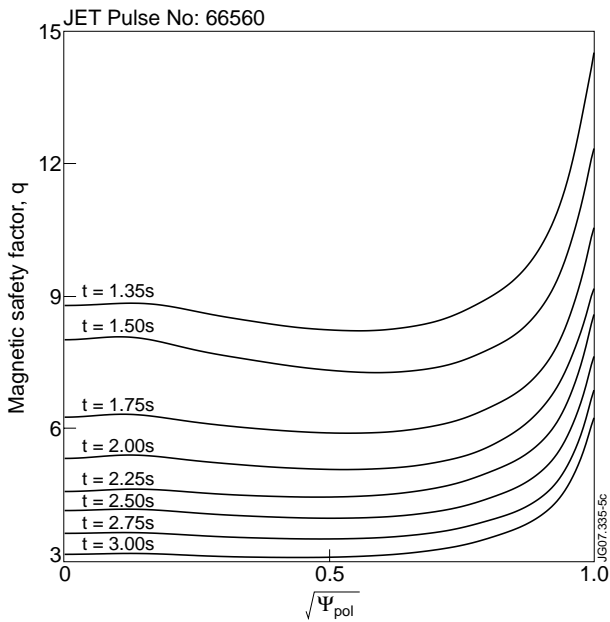


Figure 5: q profiles at various times during the current ramp as function of the normalized poloidal flux coordinate ($\sqrt{\Psi_{pol}} \approx r/a$).

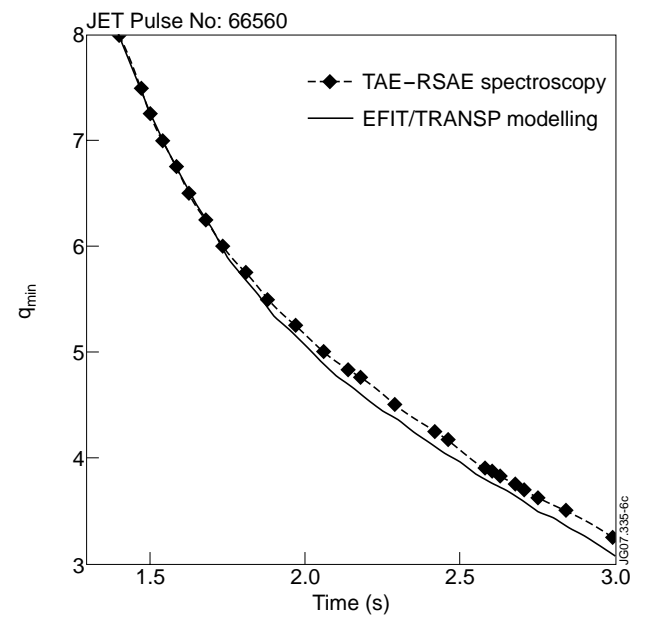


Figure 6: Evolution of q_{min} from EFIT/TRANSP (solid line) compared to the one from TAE-RSAE spectroscopy (curve with diamonds).

